Supplementary Materials

Solving Complex Open-Framework Structures from X-ray Powder Diffraction by Direct-Space Methods using Composite Building Units

A. Ken Inge[ab], Henrik Fahlquist[b], Tom Willhammar[ab], Yining Huang[c], Lynne B. McCusker[d] and Xiaodong Zou[ab]*

[a]Berzelii Center EXSELENT on Porous Materials, Stockholm University, Stockholm, SE-106 91, Sweden, [b]Department of Materials and Environmental Chemistry, Stockholm University, Stockholm, S-106 91, Sweden, [c]Department of Chemistry, The University of Western Ontario, London, N6A 5B7, Canada, and [d]Laboratory of Crystallography, ETH Zurich, Zurich, CH-8093, Switzerland

Correspondence email: xzou@mmk.su.se

Contents

Thermal and chemical analysis (TGA, *in situ* XPD and elemental analysis)

Four and a half $MPMD^{2+}$ cations are needed to counter-balance the framework charge of -9 per chemical formula unit. TGA (Fig. S1) revealed a 4.5 % weight loss from 50 to 100 °C attributed to the evacuation of eight water molecules per formula unit (calc. 4.6 %). From 200 °C to 600°C three steps of weight losses were observed with a total loss of 15.3 %. This is attributed to the loss of H_2MPMD molecules (calc. 15.0%). SU-66 was stable in vacuum up to 150 °C as determined by *in situ* XPD (Fig. S2). From 200 °C to 350 °C, the crystallinity was observed to degrade. At 400 °C the material became completely X-ray amorphous. Thus the framework of SU-66 is stable upon removal of water but crystallinity is lost upon full removal of H_2MPMD. Elemental analysis indicated wt % of C 10.96, N 3.50 and H 4.56 (atomic ratio C:N:H=2.80:1:10.67), in relatively good agreement with the values expected for $4.5C_6H_{18}N_2^{2+}$ and eight water molecules as guest species (calc. wt % C 10.28, N 3.10, H 4.00 with atomic ratio of 3:1:10.78).

Ga solid-state NMR

To gain information on the coordination geometry around gallium, Ga solid-state NMR (SSNMR) experiments were performed. Gallium has two NMR active isotopes: ^{71}Ga and ^{69}Ga (both of which have a spin of *3/2*) with natural abundances being 40 and 60 %, respectively. $^{71/69}Ga$ SSNMR spectra are usually dominated by quadrupolar interaction, yielding very broad signals. Comparing with ^{69}Ga, ^{71}Ga has a larger gyromagnetic ratio (γ) and a much (60%) smaller quadrupole moment and therefore is often the choice for Ga SSNMR in spite of its smaller natural abundance. Since the Ga concentration in SU-66 is very low, we acquired ^{71}Ga SSNMR spectra at ultrahigh magnetic field of 21.1 T to increase the sensitivity and reduce the second-order quadrupolar broadening. Fig. S1 shows the ^{71}Ga MAS NMR spectrum which contains a single peak. The isotropic chemical shift of this resonance is 169 ppm. Previous work has established the correlations between ^{71}Ga chemical shift and local Ga geometry (Bradley *et al.*, 1993, Ash & Grandinetti, 2006, Massiot *et al.*, 1999) in various Ga containing oxides. The observed ^{71}Ga chemical shift falls in the range for tetrahedral GaO_4 environment, indicating unambiguously that in SU-66, Ga only occupies tetrahedral sites. Although the sample is highly crystalline as indicated by the XPD pattern, the observed signal due to central transition does not have a typical lineshape arising from the second-order quadrupolar interaction in a crystalline phase. The resonance is asymmetrically broadened with a tail at the low-frequency side, indicating a distribution of quadrupolar coupling constants due to a range of slightly different Ga environments. The disordering likely originates from the variation in the types of atoms occupying the second-coordination sphere. Specifically, the NMR result indicates the existence of $Ga(OGe)_x(OGa)_{4-x}$ (x = 0-4) environments (with x being close to 4 due to the very low Ga content). A similar situation was also found in gallium analogue zeolites (Timken & Oldfield, 1987). Furthermore, the Ge in the

second-coordination sphere of gallium can be octahedral and/or tetrahedral. Since the spectrum is dominated by the quadrupolar interaction which is sensitive to the long-range ordering, the observed lineshape reflects the disordering in the second-coordination sphere mentioned above.

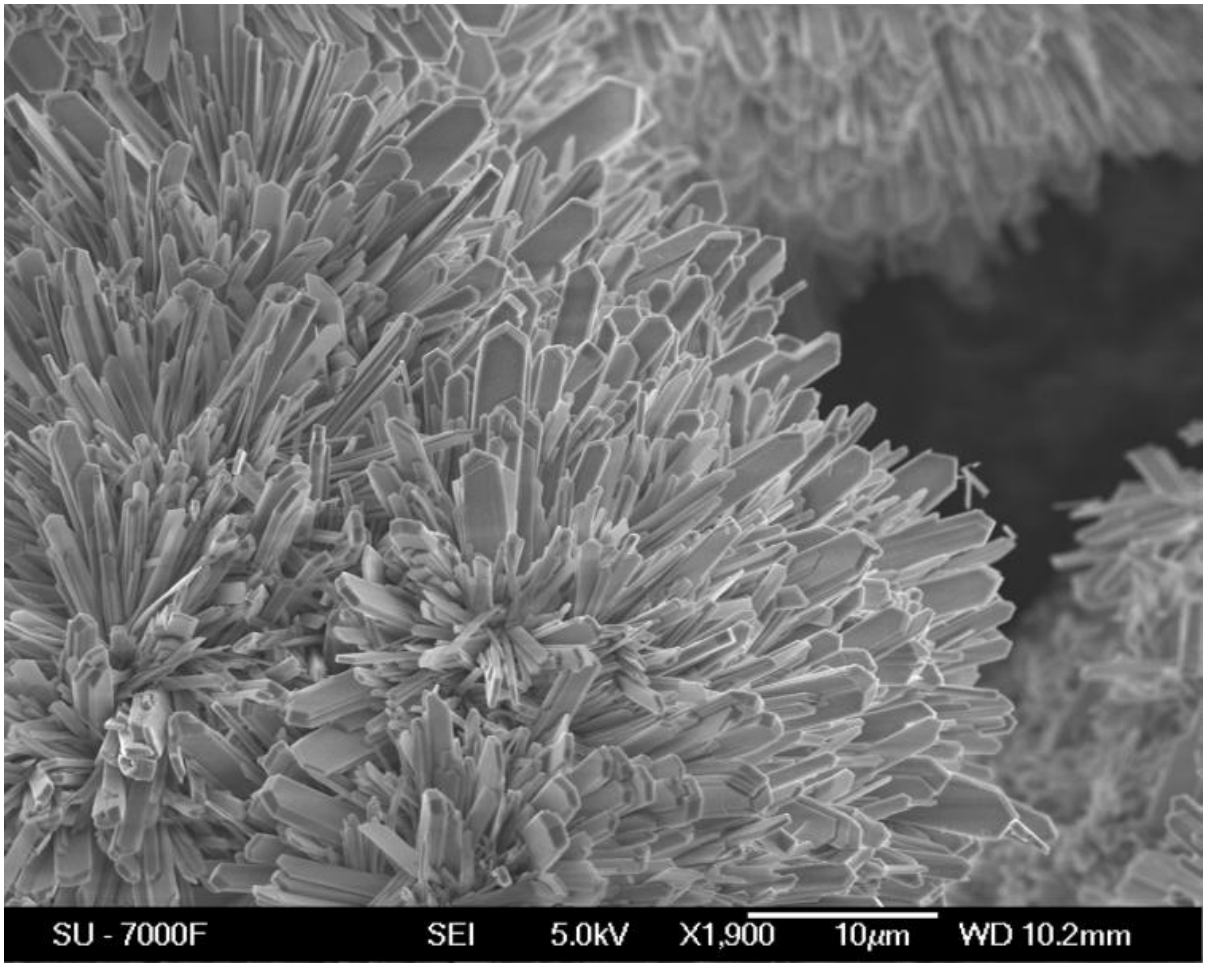

Figure S1 SEM of agglomerates of SU-66 crystals.

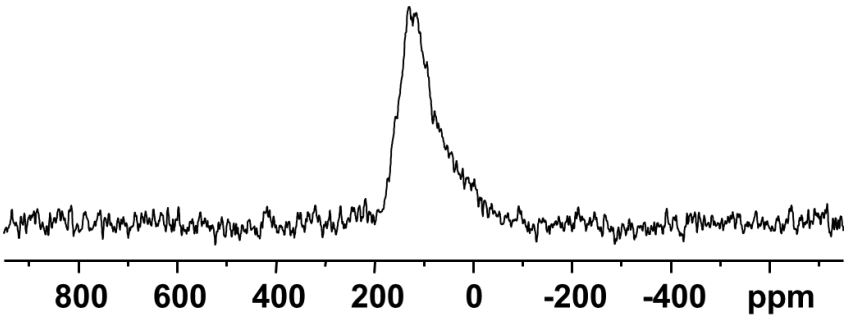

Figure S2 ^{71}Ga MAS NMR spectrum of SU-66. The sample was spun at 31.25 kHz. The number of transients is 100,000 with 0.5 s pulse delay resulting in an acquisition time of 13.9 hours.

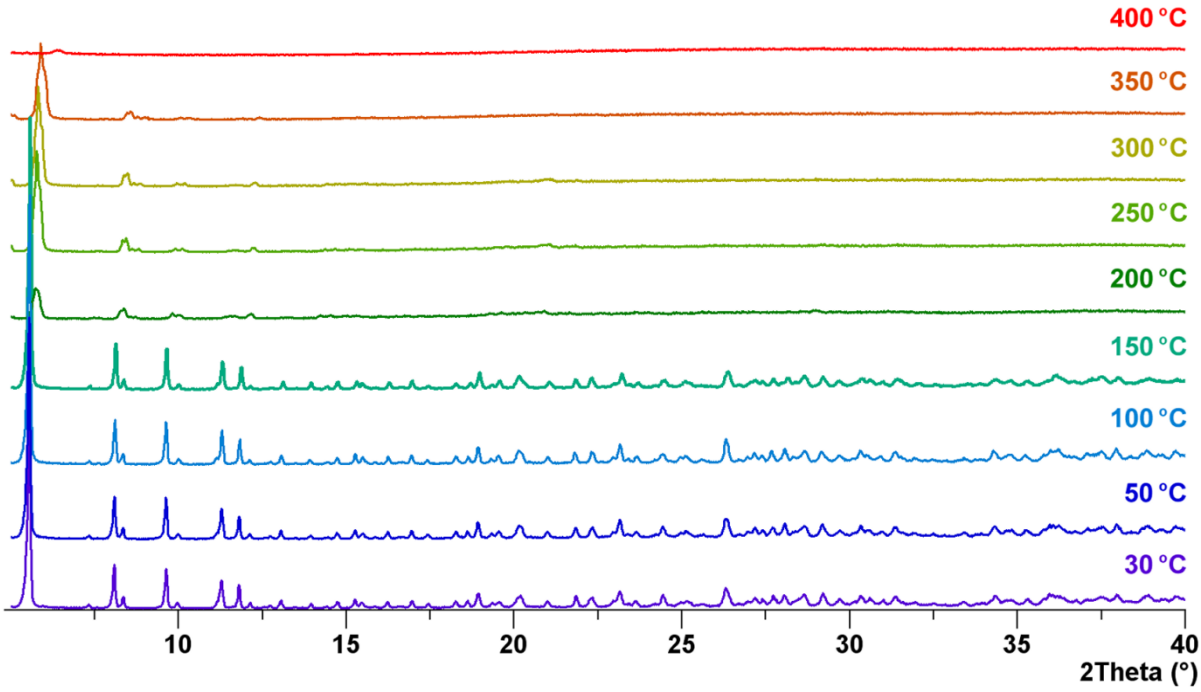

Figure S3 *In situ* XPD patterns of SU-66 recorded under vacuum.

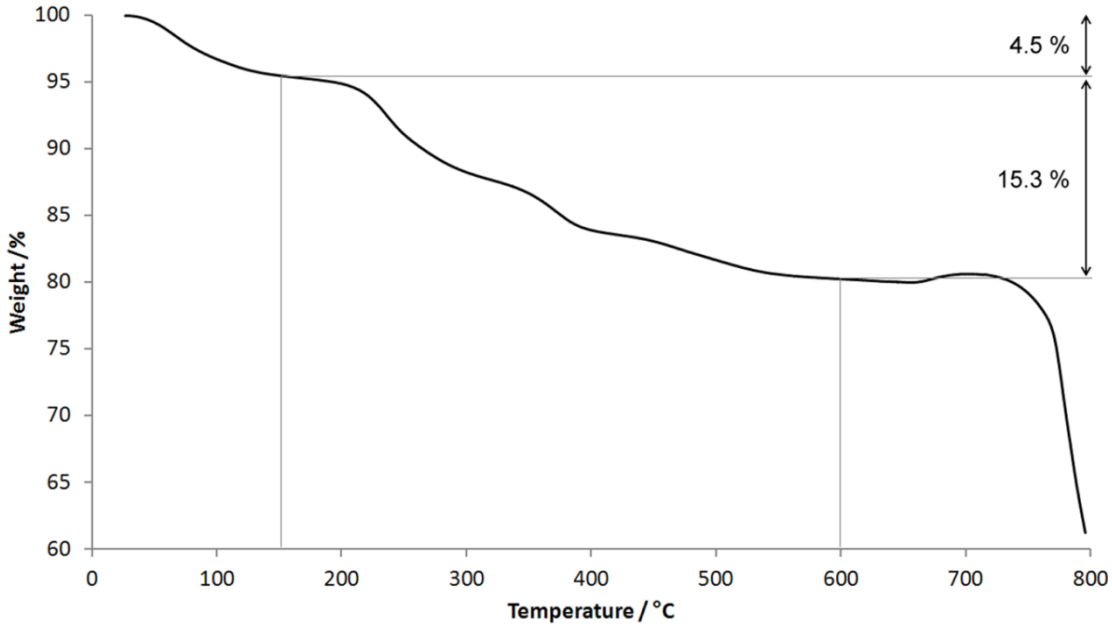

Figure S4 Thermogravimetric plot of SU-66 recorded under nitrogen atmosphere. Weight loss is attributed to the loss of water below 150 °C and organic guest species up to 600 °C.

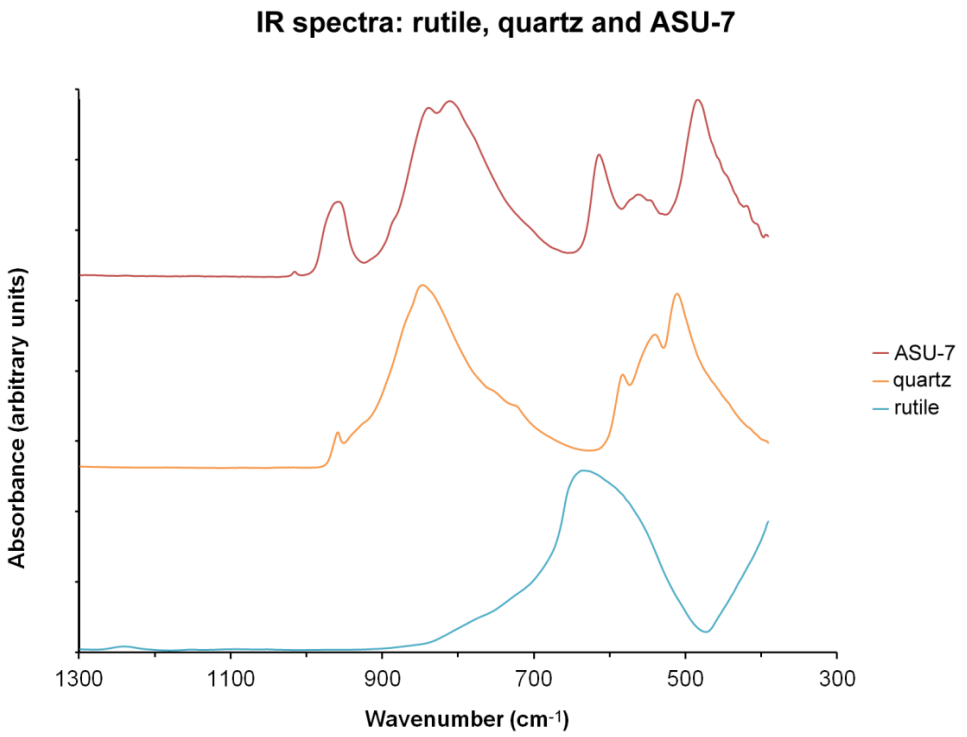

Figure S5 IR spectra between 389-1300 cm^{-1} of zeolitic germanate ASU-7 and dense GeO_2 in the quartz and rutile forms with germanium in tetrahedral and octahedral coordination environments with oxygen respectively.

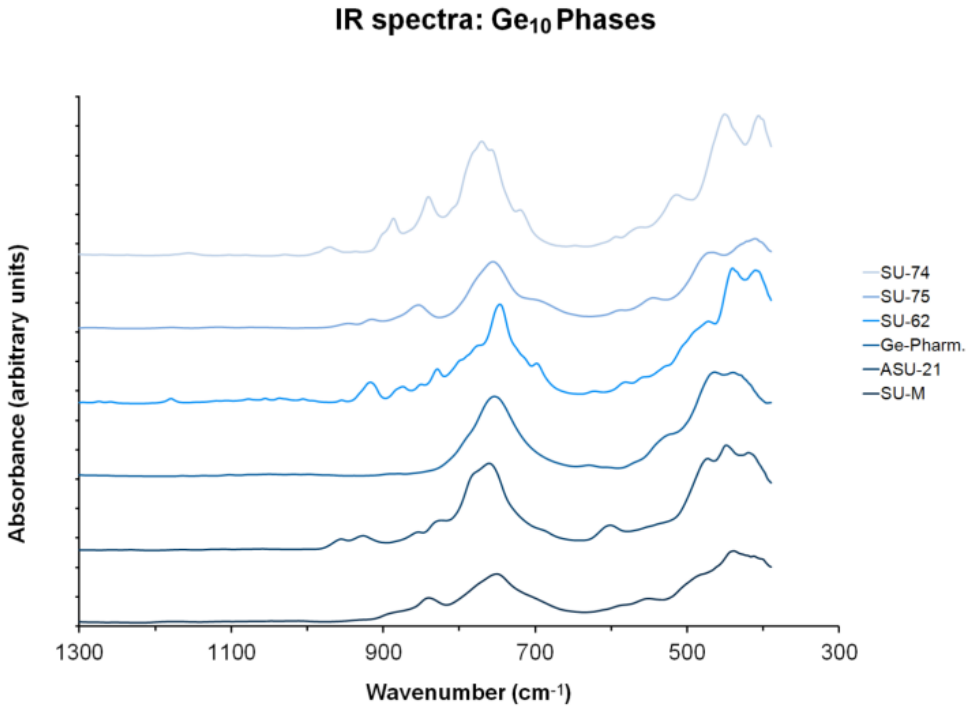

Figure S6 IR spectra between 389-1300 cm^{-1} of frameworks built of Ge_{10} clusters. Ge-Pharm. = germanium pharmacosiderite.

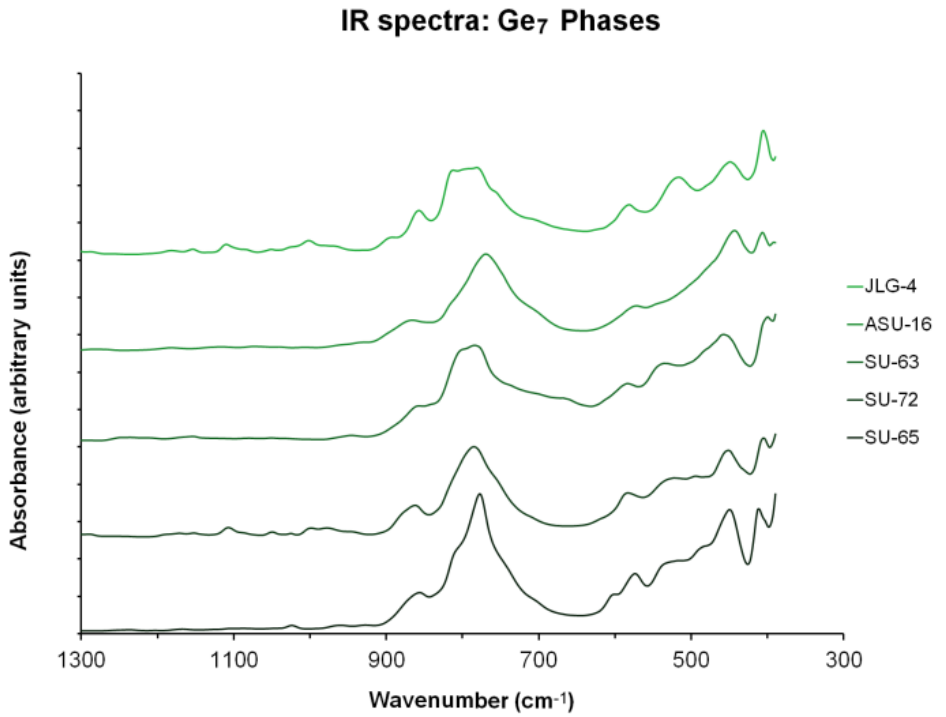

Figure S7 IR spectra between 389-1300 cm^{-1} of frameworks built purely of Ge_7 clusters.

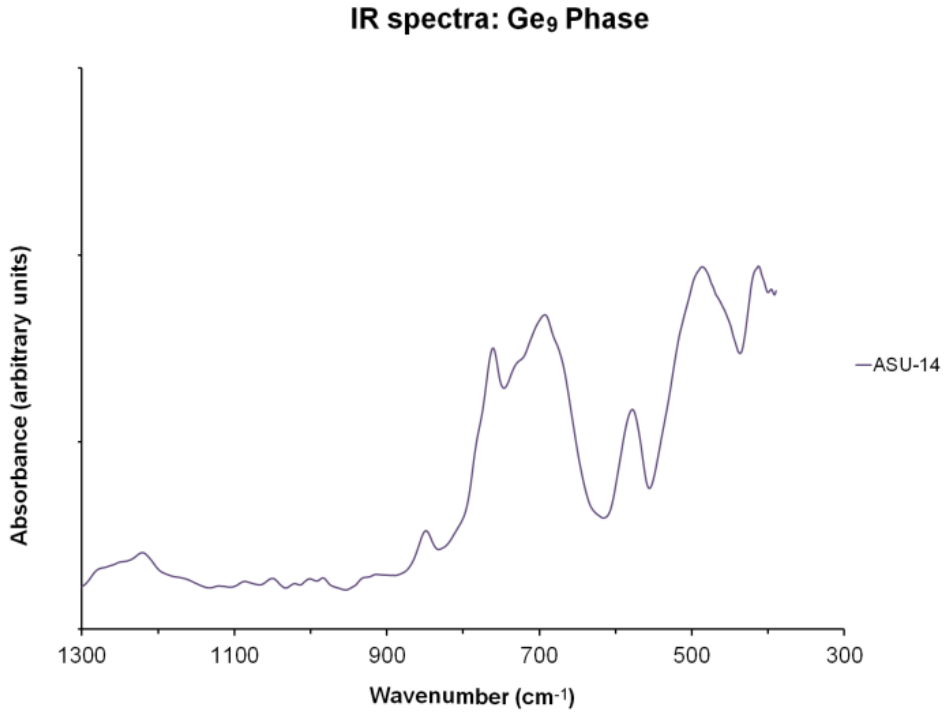

Figure S8 IR spectrum between 389-1300 cm^{-1} of ASU-14 a framework built from Ge_9 clusters only.

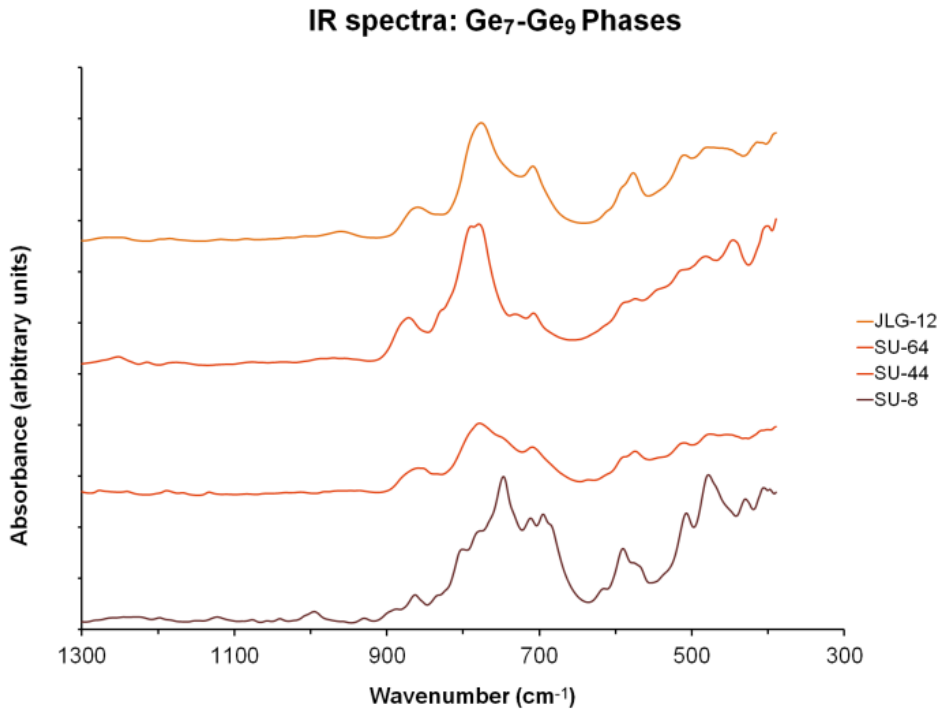

Figure S9 IR spectra between 389-1300 cm^{-1} of frameworks built of a combination of Ge_7 and Ge_9 clusters.

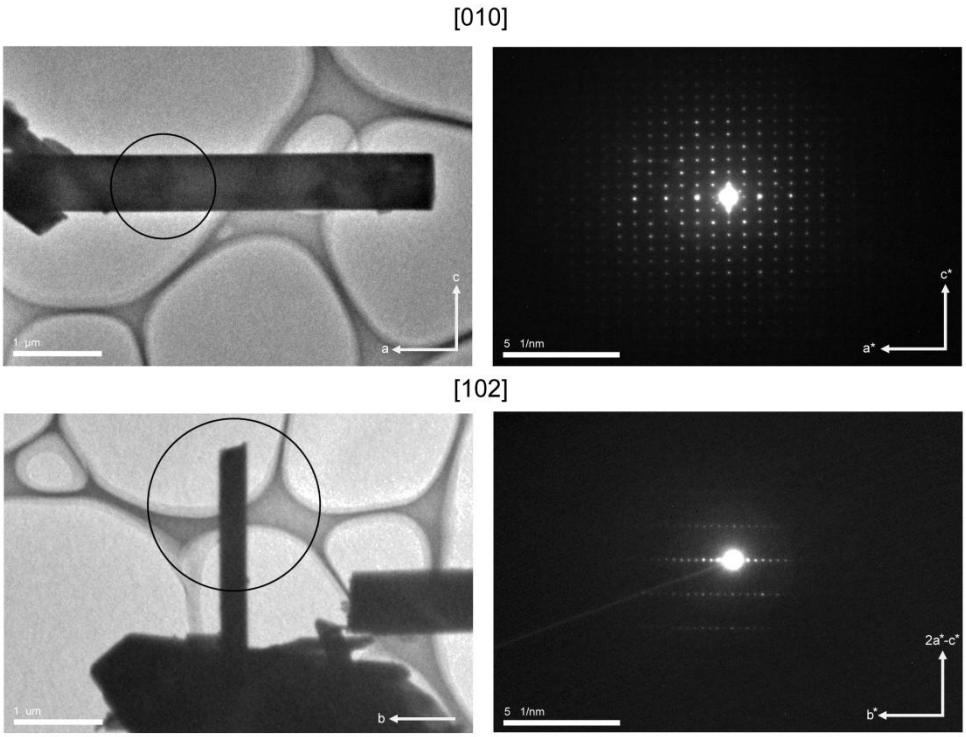

Figure S10 TEM images and SAED patterns of SU-66 along [010] and [102]. The selected areas for electron diffraction are outlined in a black circle.

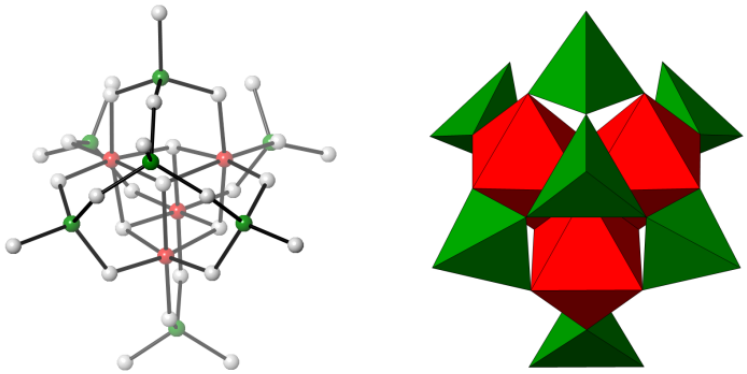

Figure S11 (Left) The Ge_{10} cluster with the apical tetrahedron in ball-and-stick and (right) polyhedral representations used to create the Fenske-Hall Z-Matrix for the structure determination of SU-66. Germanium in tetrahedral and octahedral coordination environments are shown in green and red, respectively. Oxygen atoms are shown in white.

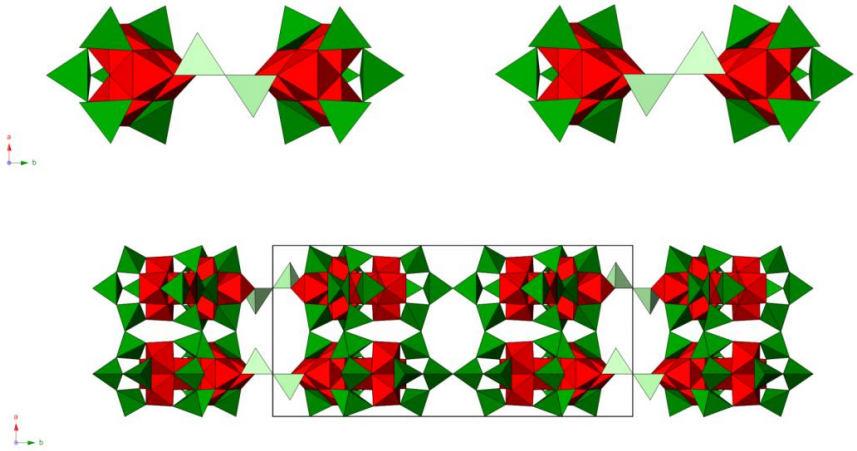

Figure S12 (Top) Disorder between two Ge_{10} clusters. The disordered tetrahedral positions are shown in light green, and each position has occupancy of one half. The two possible configurations are shown on the left and right. (Bottom) The same disorder shown across two unit cells.

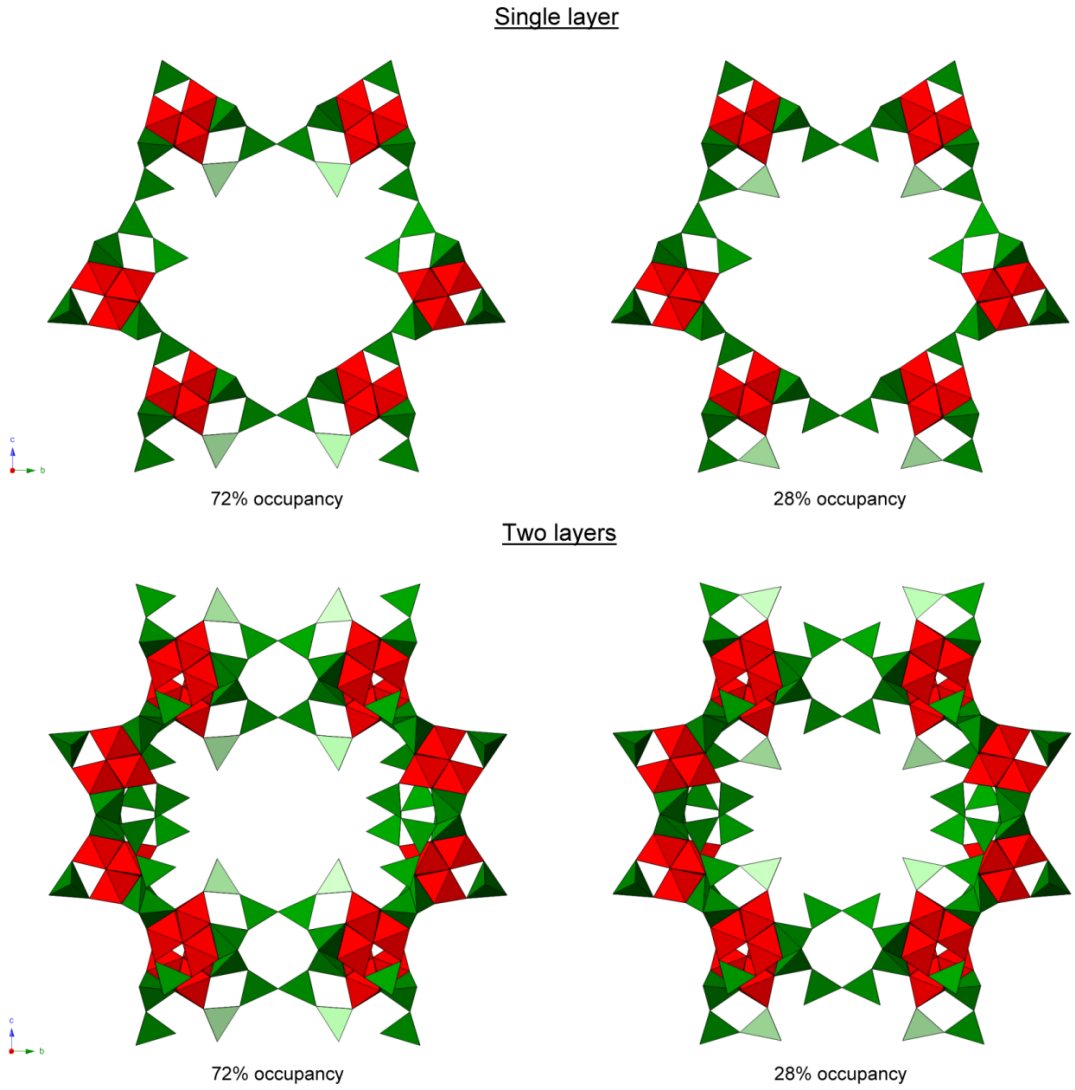

Figure S13 Positional disorder in the framework of SU-66 with the disordered tetrahedra shown in light green. The configuration on the left and right have occupancies 0.28 and 0.72 respectively. One and two layers of Ge_{10} clusters are shown on top and bottom, respectively.

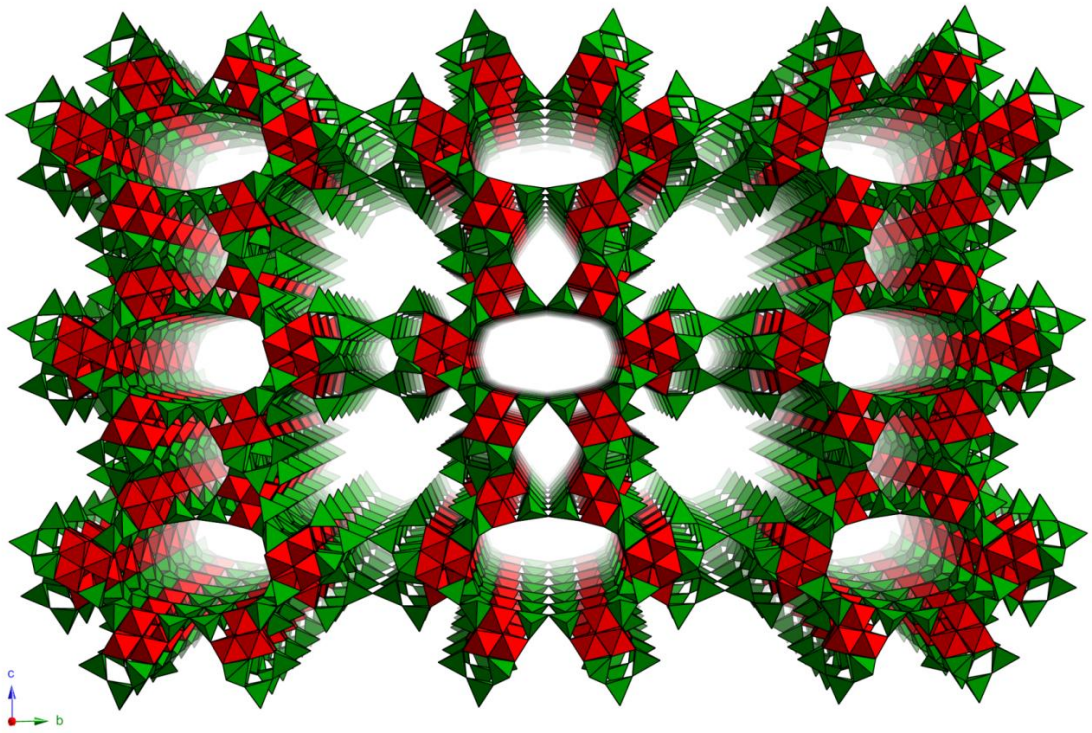

Figure S14 The framework structure of SU-66 with one-dimensional 26-, 18-, 12- and 8-ring channels, shown in polyhedral representation. Tetrahedra and octahedra are shown in green and red, respectively.

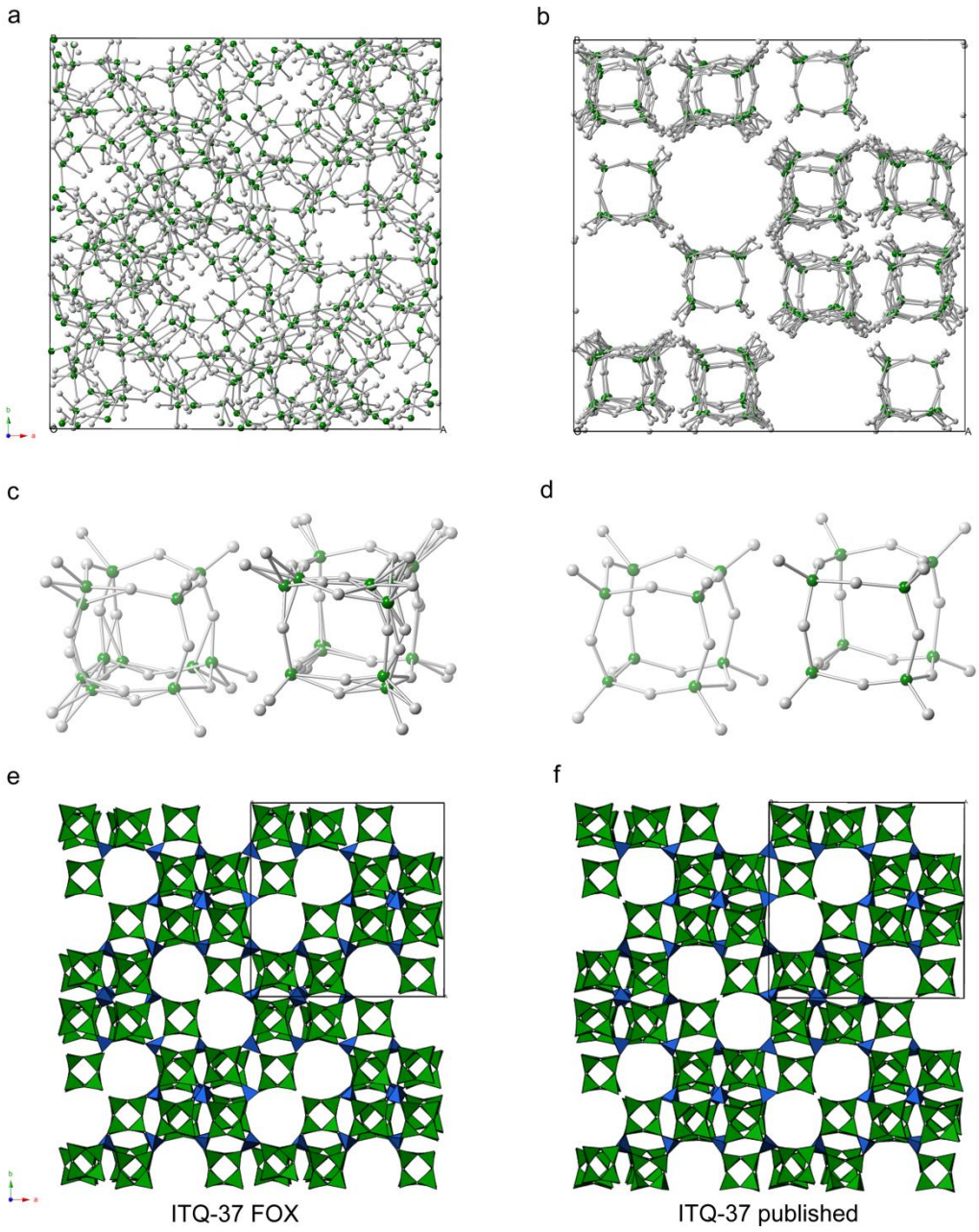

Figure S15 Structure determination of ITQ-37 by FOX. (a) Two *d*4*r*s are inserted into the asymmetric unit with a random starting position and orientation. (b) Structure solution as produced by FOX with some duplicate atoms, resulting from the application of symmetry, that have not exactly merged. (c) Two unique *d*4*r*s with redundant atoms that have not quite merged. (d) The average positions of redundant atoms have been kept. (e) Two additional tetrahedra, shown in blue, are added in the tetrahedral holes where electron density was found in the difference Fourier map. This can be compared with (f) the refined framework structure of ITQ-37 solved by combining SAED with XPD.

References

Ash, J. T. & Grandinetti, P. J. (2006). *Magn. Reson. Chem.* **44**, 823-831.
Bradley, S. M., Howe, R. F. & Kydd, R. A. (1993). *Magn. Reson. Chem.* **31**, 883-886.
Massiot, D., Vosegaard, T., Magneron, N., Trumeau, D., Montouillout, V., Berthet, P., Loiseau, T. & Bujoli, B. (1999). *Solid State Nucl. Magn. Reson.* **15**, 159-169.
Timken, H. K. C. & Oldfield, E. (1987). *J. Am. Chem. Soc.* **109**, 7669-7673.